Assessment of Groundwater Potential Zones Using Electrical Resistivity in Muzaffargarh

Warda Syed[1], Sawaid Abbas[1,2*], Muhammad Usman[1], Perveiz Khalid[3], Shahid Ghazi[1,3]
[1]Smart Sensing for Climate and Development, Center for Geographical Information System, University of the Punjab, Lahore, Pakistan
[2]Department of Land Surveying and Geo-Informatics, The Hong Kong Polytechnic University, Hong Kong SAR
[3]Institute of Geology, University of the Punjab, Lahore, Pakistan
***Correspondence:** sawaid.gis@pu.edu.pk; Tel.: +92-300-4641319

Citation | Syed. W, Abbas. S, Usman. M, Khalid. P, Ghazi. S, "Assessment of Groundwater Potential Zones Using Electrical Resistivity in Muzaffargarh", IJIST, Special Issue pp 270-286, June 2024
Received | June 01, 2024 **Revised |** June 08, 2024 **Accepted |** June 12, 2024 **Published |** June 17, 2024.

The study integrates Earth observation and geospatial data to evaluate groundwater potential and conditions in Muzaffargarh, South Punjab, Pakistan, a region grappling with freshwater scarcity due to high sediment concentrations in subsurface water. The developed approach aims to enhance sustainable water resource management in areas affected by such sediment challenges. An electrical resistivity survey was conducted at 40 locations within the study area, incorporating Vertical Electrical Sounding (VES) and spatial analysis with hydrogeological parameters to analyze and visualize the spatial distribution of freshwater. A weighted overlay analysis was employed to map freshwater and saline water zones, supported by 2D resistivity maps. The study generated several thematic layers, including data on geology, rainfall, lineaments, land use/land cover (LULC), drainage density, soil type, and slope. A groundwater potential (GWP) zone map was created, categorizing the area into four zones: very good, good, moderate, and poor. Additionally, resistivity maps were produced at depths of 2m, 10m, 50m, 80m, 200m, and 300m to analyze resistivity variations in the Ghazi Ghat and Qasba Gujrat areas of Muzaffargarh district. The study's findings include curves indicating potential groundwater zones and a comprehensive understanding of subsurface characteristics through resistivity curve comparisons. These results provide valuable insights for the sustainable management of groundwater resources in the region, particularly in addressing freshwater scarcity.

Keywords: Electrical Resistivity Survey, Vertical Electrical Sounding, Google Earth Engine, Groundwater Potential Zone.

Introduction:

A region's socioeconomic development and urbanization are heavily influenced by its sustainable freshwater supply [1]. Water's ability to dissolve, suspend, and adsorb a variety of pollutants, including organic and inorganic substances like arsenic, sulfides, and chlorides, is due to its high solubility [2]. Pakistan faces significant freshwater shortages, primarily due to its arid to semi-arid climate and limited precipitation. Consequently, the population depends heavily on groundwater for industrial, agricultural, and domestic needs. Groundwater contamination primarily results from poor solid waste disposal practices, while excessive extraction contributes to rising salinity levels [3]. Groundwater, which fills pore spaces in soil and fractures in rock formations, is a vital resource supporting biodiversity, economic growth, and human health. Its occurrence and movement depend on various factors, with the hydrological cycle maintaining an equilibrium where inflow equals outflow, resulting in minimal net change [4][5]. Given the random distribution of global water resources, effective scientific methods are crucial for identifying potential aquifer zones for replenishment and use. Geophysical methods, including the Electrical Resistivity Method (ERM), are employed to investigate groundwater. ERM has long been used for mapping geological environments and assessing the thickness of layered media. Its ease of use, effectiveness, and non-destructiveness make it a preferred method for groundwater studies. Groundwater potential zonation assesses an area's groundwater potential using both quantitative and qualitative methods, employing surface and subsurface indicators. Subsurface data is gathered via observatory wells, electrical resistivity techniques, and direct observations, while surface features are accessed through remote sensing and field verification. Electrical resistivity sounding offers an indirect method for interpreting subsurface geological conditions, particularly in lineaments and weathered rock zones. Vertical electrical sounding (VES) is widely used due to its cost-effectiveness and suitability for deep probing.

The integration of remote sensing, Geographic Information Systems (GIS), and electrical resistivity has revolutionized groundwater resource assessment and management. These technologies are essential for locating and characterizing potential groundwater zones, with GIS enabling the integration, analysis, and visualization of spatial data. Electrical resistivity directly probes geological formations to assess their groundwater storage and transmission capacity. This integrated approach allows for accurate identification, delineation, and assessment of freshwater potential zones, supporting sustainable groundwater management. The study aims to assess and delineate groundwater potential zones in Muzaffargarh, South Punjab, Pakistan, addressing the region's freshwater scarcity due to high sediment concentrations. The research develops a sustainable water resource management approach, involving an electrical resistivity survey at 40 locations, integrating Vertical Electrical Sounding (VES) and spatial analysis with hydrogeological parameters. A weighted overlay analysis maps fresh and saline water zones using 2D resistivity maps. The study also seeks to determine water depth and quality at various levels, identify freshwater zones in the subsurface, and create a comprehensive groundwater potential map by integrating remote sensing, GIS, and electrical resistivity data.

Material and Methods:

Description of Study Area

Muzaffargarh is an agricultural district located in Punjab, Pakistan, positioned between 29° 6' to 30° 45' N latitude and 70° 30' to 71° 48' E longitude. It is centrally situated between the Chenab and Indus rivers. The district encompasses four tehsils: Alipur, Jatoi, Kot Addu, and Muzaffargarh. Spanning a total area of 830,000 hectares, Muzaffargarh is connected by 1,084 km of metalloid roads to neighboring districts such as Multan, Rajanpur, D.G. Khan, and Rahim Yar Khan. Within this area, 112,700 hectares are affected by salinity, and 1,170 hectares are waterlogged. According to the 1998 census, the district had a population of 2,635,903 [18]. Thal Doab, a triangular region bordered by the Indus River to the west and the Chenab River to the east, covers an area of 7.9 million acres [19][20]. Our study area, situated in Thal Doab within

Muzaffargarh, has an average elevation of approximately 122 meters above sea level and lies along the southern bank of the Chenab River [21]. The hydrology of the region faces several critical issues, including water scarcity and contamination. Persistent water shortages and poor water quality, due to contamination, have long been concerns for local residents. The area experiences minimal annual rainfall, which exacerbates soil salinity problems. The primary objective of this study is to identify significant freshwater aquifers and regions with contaminated subsurface water to address these pressing challenges.

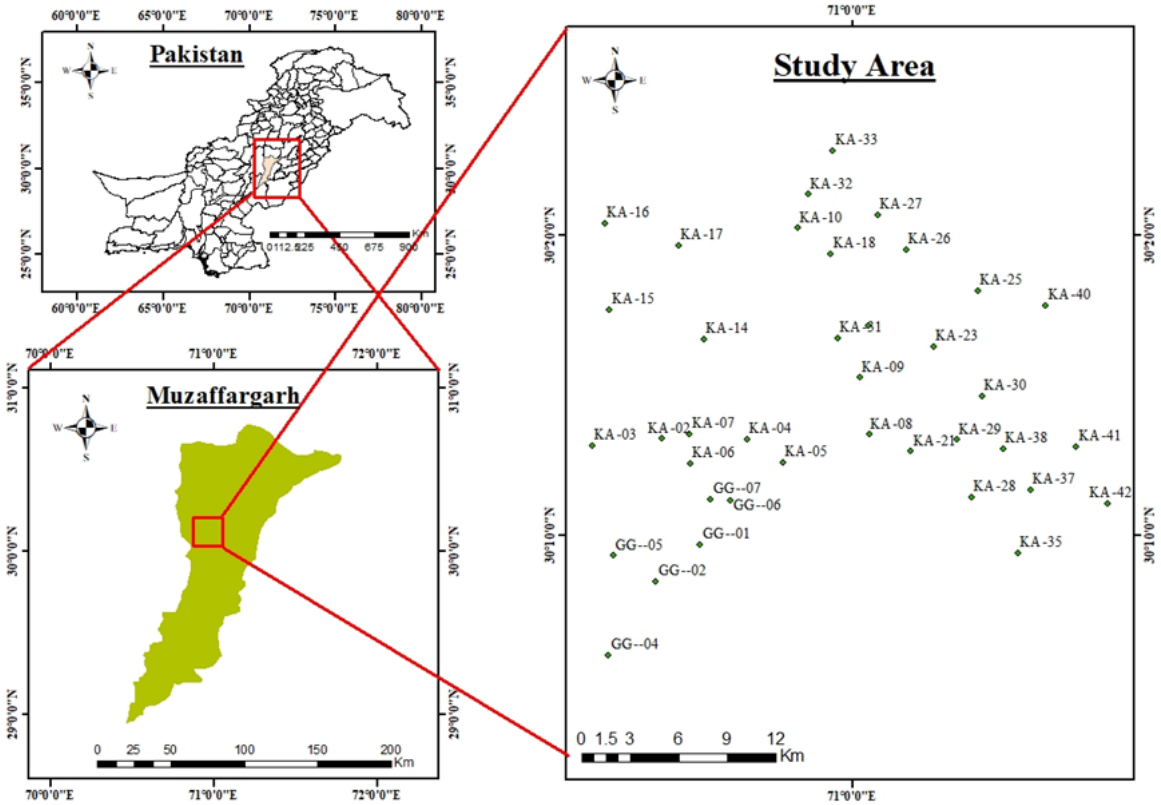

Figure 1: Map showing the location of the study area and distribution of ground survey points in southern Punjab Pakistan

Geology of Muzaffargarh:

The district of Muzaffargarh is classified into various lithological units based on a geological map published by the Geological Survey of Pakistan (GSP, 1964), compiled by M. Abu Bakr, M.S.C. from the Geological Survey of Pakistan, and Roy O. Jackson from the U.S. Geological Survey. The research area falls within the Central Indus Basin and is primarily composed of Quaternary deposits. These deposits are categorized as follows: Eolian sand of the Thar Desert or dune sand deposits (Qs), floodplain deposits or eolian sand deposits, deposits of extinct streams with relief less than 100 feet (Qsc), stream-bed and meander-belt deposits (Qm), and active floodplain deposits (Qf).

Data Collection:

An electrical resistivity survey was conducted to estimate water quality in the Thal Desert area, which primarily consists of clay, sand, silt, and silty clay. The Schlumberger configuration was used for this survey, where electrodes are arranged in a straight line to form a circuit. In this configuration, the distance between the inner electrodes remains constant, while the distance between the outer electrodes is varied at each Vertical Electrical Sounding (VES) point. The Schlumberger configuration requires that the current electrode spacing be greater than or equal to the distance between the inner electrodes. Certain conditions must be met before initiating the resistivity survey to ensure accurate results.

$$AB \geq 5MN \quad (1)$$

- Resistivity contrasts should be evident among the formations being examined.
- If the surface consists of alternating thin layers, the measured resistivity reflects the average effect of these layers.
- The resistivity array should be positioned away from electrical lines in the field. If electrical lines are close to the investigation point, the array should be oriented perpendicularly to these lines to prevent electrical interference from affecting the resistivity measurements and introducing noise.

Using the Schlumberger configuration, approximately 40 Vertical Electrical Sounding (VES) points were established. At each VES point, the AB/2 distances used were 1.5, 2, 3, 4, 6, 8, 10, 15, 20, 25, 30, 40, 50, 60, 80, 100, 125, 150, 200, 250, and 300 meters. The AB/2 distance was adjusted at each VES point, and when the Schlumberger configuration began yielding low resistivity values, the MN distance was also modified. Upon completing the circuit, a current of 200 mA was introduced into the ground, which was then measured by potential electrodes to determine the resistivity values. The resistivity meter was used to measure resistance in ohmmeters. The primary objective of this survey was to calculate apparent resistivity, which represents the average resistivity of subsurface materials. Apparent resistivity was calculated using resistance and a geometric constant (K), both of which were derived from field measurements.

$$\rho_a = R*K \quad (2)$$

- ρ_a = apparent resistivity
- K= geometric constant
- R = resistance offered by ground
- R is calculated by using the given formula

$$R = \frac{V}{I} \quad (3)$$

- R = resistance
- V = Potential difference
- I = electric current

Geometric factor K was calculated by using the given formula

$$K = \pi * \frac{(AB/2)^2 - (MN/2)^2}{MN} \quad (4)$$

- AB = distance between outer current electrodes
- MN = distance between inner potential electrodes

Apparent resistivity was calculated using the specified formulas, and values for all parameters were plotted to create graphs of apparent resistivity. These graphs were plotted with AB/2 on the x-axis and apparent resistivity (ϱa) on the y-axis. After generating graphs for each VES point and compiling them into a Word document, the data were further processed using the software IPI2WIN. This software generates synthetic curves that correspond to the field resistivity curves. The field resistivity curves, derived from field-acquired data, were compared with synthetic curves produced by minimizing potential errors.

The models generated by IPI2WIN were utilized to determine the thickness and depth of geological layers. The software's table window displays the Root Mean Square (RMS) error, which should be less than 1%. To achieve this, adjustments were made to the apparent resistivity (ϱa), resulting in changes to the RMS value. Several models produced by IPI2WIN are shown in Figure 6, where red curves represent synthetic or best-fit curves, while black curves depict field data. The blue layers indicate lithological units, with layer identification achieved through analysis of these curves. Vertical Electrical Sounding (VES) is a reliable, non-destructive method

for groundwater exploration, requiring specific conditions to ensure accuracy. Its effectiveness can be further validated by correlating results with borehole data. Despite its reliability, VES has a limitation: it necessitates a long array of wires, which can be challenging to manage during data collection from deep resources. Nonetheless, the method's overall reliability mitigates this limitation.

$$CR = \frac{CI}{RI} \quad (5)$$

Where RI denotes the Random Index, CI represents the Consistency Index, and CR stands for the Consistency Ratio. A CR value of ≤ 0.10 is considered acceptable, with a CR of 0 indicating a perfect level of consistency. The groundwater potential zone map for Muzaffargarh was developed by integrating all seven thematic maps through a weighted overlay assessment approach on a GIS platform, utilizing an algorithm to combine the data effectively.

Research Methodology:

In this study, various spatial analysis techniques in ArcGIS were utilized to process and evaluate integrated datasets. This involved creating derivative maps and performing spatial overlays to identify relationships and patterns among variables (Figure 2).

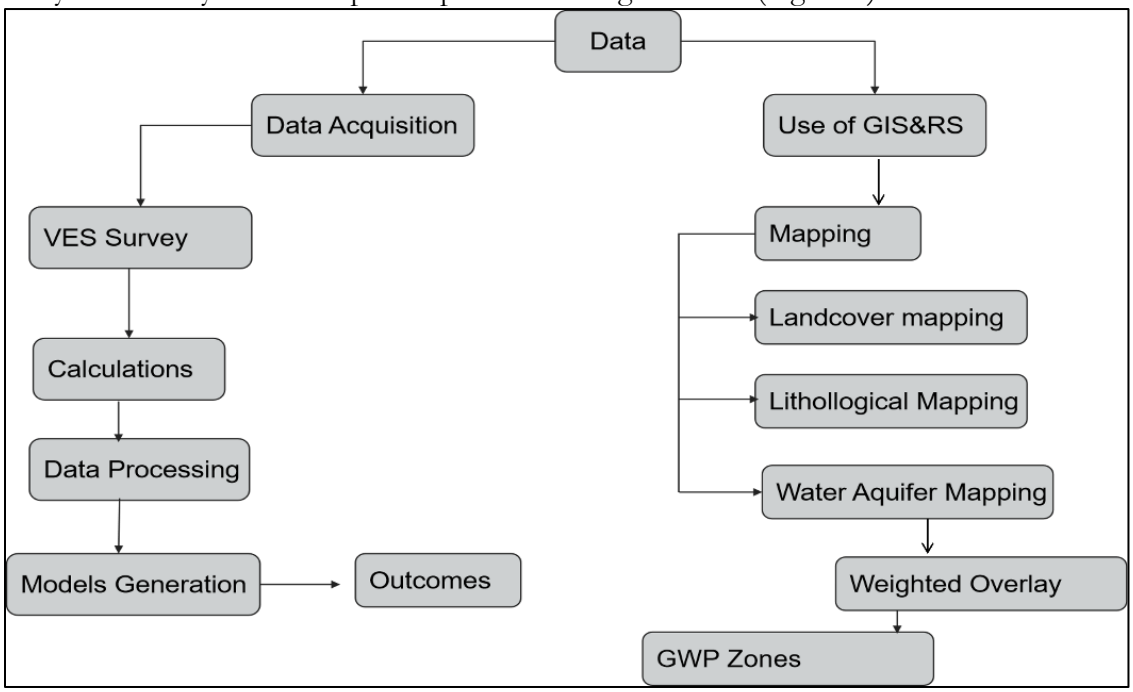

Figure 2: Flow chart indicating the step-by-step procedure adopted in the study

Remote sensing (RS) and GIS methods were employed for hydrological investigations of drainage basins, addressing various aspects of the physical environment within the basin and its surroundings. These techniques are particularly crucial in arid regions facing issues like limited freshwater resources and frequent flash floods. RS and GIS facilitated the extraction of hydrological data for both qualitative and quantitative assessments of drainage system parameters in dryland environments.

The study incorporated various geospatial datasets, including Digital Elevation Models (DEM) from the Shuttle Radar Topography Mission (SRTM) sourced from the USGS website, as well as field surveys, soil types, water table depth, and geological data. These datasets were processed using ArcGIS version 10.5 to analyze factors such as DEM, land use, soil types, geomorphology, hill shade, and drainage density. Thematic maps, including geology, drainage density, soil, land use/land cover (LULC), rainfall, lineament density, and slope, were created to estimate recharge potential and groundwater potential zones in the study area. The soil map was prepared using data from the "Soil Grids" website, LULC data was directly downloaded from

the ESRI website, and the rainfall map was compiled from data available on "Cru data." The geology map was digitized based on information from the Geological Survey of Pakistan, while other maps were generated using DEM data.

Additionally, the study aimed to utilize Electrical Resistivity Surveys to determine subsurface layers through the Inverse Slope method using IPI2WIN software. Satellite data was also employed for map creation. Electrical resistivity surveys, a widely used geophysical method for groundwater prospecting and hydrogeological investigations, are effective in areas where resistivity contrasts are present among surrounding formations and water-bearing strata. This technique helps determine the thickness and resistivity of layered media to locate groundwater aquifers. Vertical Electrical Sounding (VES), which employs four electrodes—two current electrodes (A and B) and two potential electrodes (M and N)—is used to measure resistivity. The Schlumberger electrode configuration, as illustrated in Figure 3, was utilized, with current electrodes injecting current into the ground and potential electrodes measuring the resultant potential difference.

Table 1: AHP matrix indicating weight for each layer

Matrix		Rainfall	Geology	Slope	Drainage Density	LULC	Lineament Density	Soil	**Normalized Principal Eigenvector**
		1	2	3	4	5	6	7	
Rainfall	1	1	2	1	5	1	3	6	25.38%
Geology	2	1/2	1	1	5	2	2	6	21.79%
Slope	3	1	1	1	2	1	1	4	15.70%
Drainage Density	4	1/5	1/5	1/2	1	1	2	3	9.19%
LULC	5	1	1/2	1	1	1	3	6	16.16%
Lineament Density	6	1/3	1/2	1	1/2	1/3	1	4	8.75%
Soil	7	1/6	1/6	1/4	1/3	1/6	1/4	1	3.02%

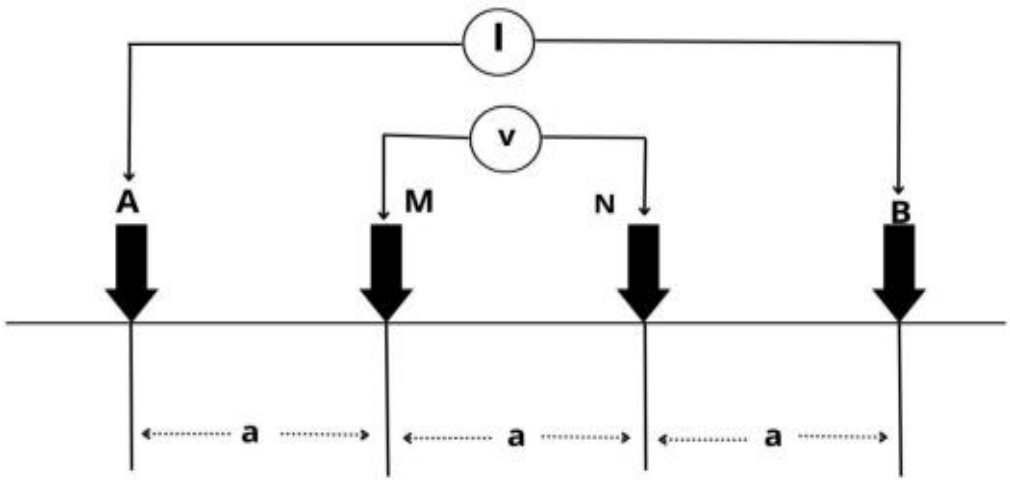

Figure 3: Illustration of electrode array using Schlumberger electrode configuration used in field during data acquisition.

The weighted overlay method in ArcGIS 10.5 was used to estimate groundwater zones by combining various thematic maps. Each layer was assigned a weight and rank, as outlined in Equation (6), where \ (A \) represents the weight of the parameter, \ (B \) is the rank of the

subclasses in each parameter map, and \(i \) and \(n \) denote the initial and final values, respectively, for the number of parameters. After determining the total normalized weights for each thematic layer and its attributes, the groundwater potential zones were delineated using the raster calculator in ArcGIS 10.8. Based on the cumulative score of the groundwater potential zones, four classes were identified: very good, good, moderate, and poor.

Results:

The research area, located in Muzaffargarh within the Central Indus Basin, is characterized by Quaternary deposits. Using ArcGIS, various layers were created to represent the area's geological and hydrological features, as detailed in Figure 4. Models generated with ground data and IPI2WIN software illustrate the subsurface lithologies and types of water present. Resistivity values were used to differentiate between materials: low resistivity values indicate clay sediments above the water table or saline water below it, while high resistivity values suggest the presence of fresh water with some sandy strata. The resistivity values for different materials are listed in Table 2. Ground data collected in the field were plotted in ArcGIS to visualize resistivity at various depths, as shown in Figure 7.

Table 2: Resistivity threshold values for various lithologies utilized in the interpretation of Vertical Electrical Sounding (VES) data.

Resistivity Zone	Resistivity Range (ohm-m)	Interpreted Lithology
Very high	Greater than 230	Coarse sand with gravels and Kanker
High	230 to 100	Sand with gravels with minor interbedded thin layers of silt and clay
Medium	100 to 40	Medium to coarse sand
Low	40 to 20	A mixture of sand with silt and clay Silty clay / clayey silt (Above GWT)
Very low	Less than 20	Saline sediments, silty clay in dominance (Below GWT)

Elevation and Slope:

The elevation of the land surface plays a crucial role in groundwater replenishment by driving water movement through gravity. By analyzing elevation data, we can identify regions that contribute to groundwater flow [23]. Elevation is a key topographic feature for assessing groundwater potential. The elevation map for the study area was developed using the SRTM DEM. Altitude influences climate variations, which in turn affect rainfall patterns and soil quality [24]. Elevation gradients impact groundwater direction and flow, while changes in landscape elevation contribute to groundwater recharge and movement. This information is vital for effective water resource management and sustainability [25]. Typically, flat land surfaces experience lower runoff compared to moderately and highly elevated areas. Runoff in flat regions ranges from 0 to 0.4%, while infiltration is generally greater in flat areas than in regions with steep or moderately steep slopes.

Soil Texture:

Land water infiltrates through the soil's voids to reach the aquifer, making soil a fundamental factor in determining potential groundwater zones. Consequently, various technologies and techniques, such as remote sensing, GIS, and AHP, are employed in groundwater research [26]. Soil type maps are created based on the average size of solid particles in the soil, including sand, silt, and clay. Soils with high infiltration rates, such as sand, gravel, and boulders, are assigned higher weights (Figure 4g).

LULC:

Land Use and Land Cover (LULC) maps were generated by classifying raster datasets for the years 2000, 2010, and 2020, as shown in Figure 4f. Seven categories were developed based on land use types for these different years.

Rainfall:

Rainfall data for the years 2011-2021 was downloaded and processed in ArcMap to create an average rainfall map, shown in Figure 4c. Geophysical methods are essential for analyzing the subsurface geology of specific areas by detecting discontinuities caused by contrasts in the physical properties of rocks. Given the complexity of geophysical patterns and the interpretation of these discontinuities, an integrated survey using two or more geophysical methods is commonly employed. This approach provides a more accurate depiction of subsurface geology and addresses challenges related to the earth's inhomogeneous nature. For this project, a geophysical survey was conducted incorporating GIS, remote sensing (RS), and electrical resistivity methods for groundwater exploration.

Groundwater Potential Zone Map:

A groundwater potential (GWP) zone map was created using thematic layers, categorizing the study area into four zones: very good, good, moderate, and poor, as shown in Figure 5.

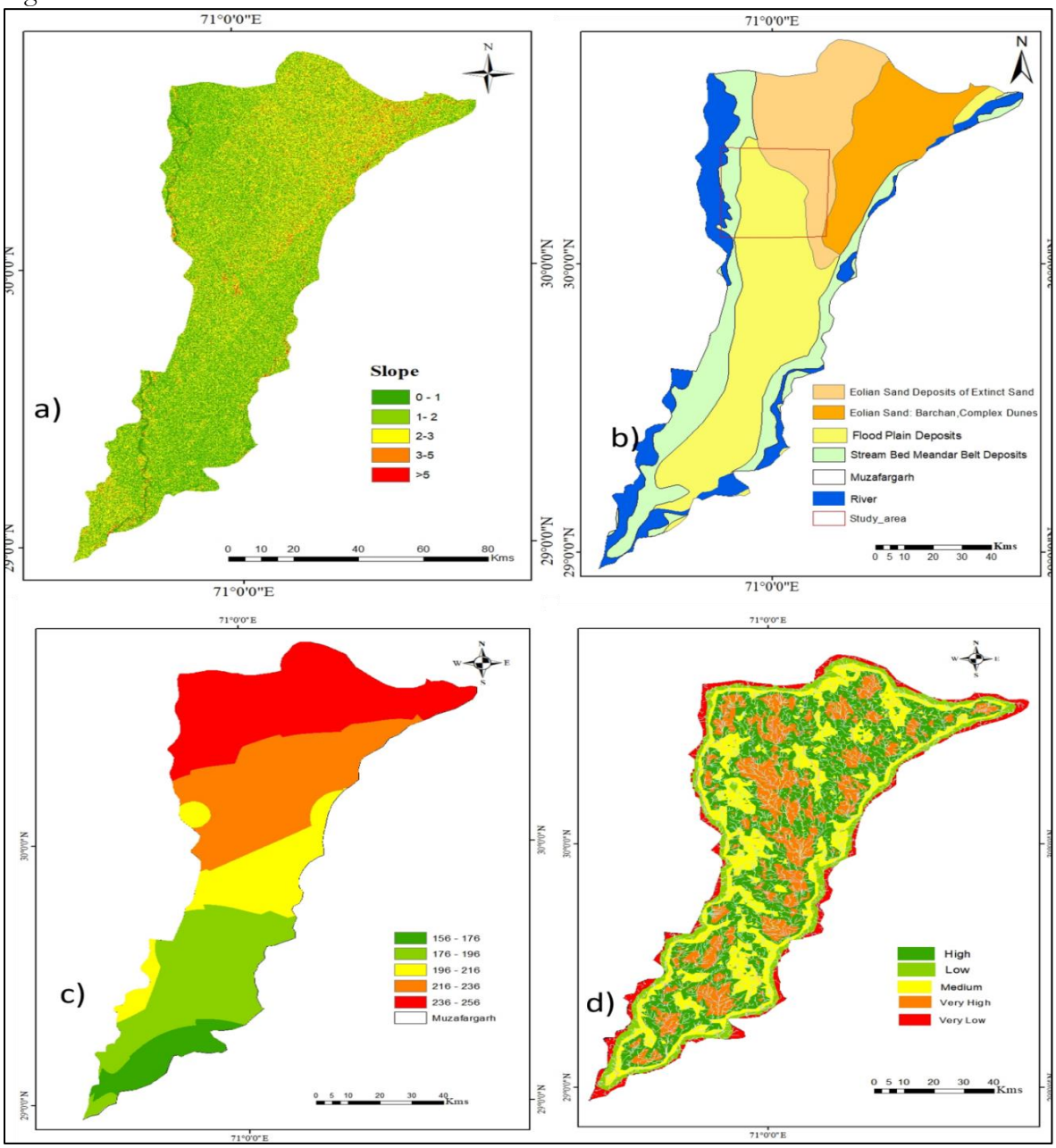

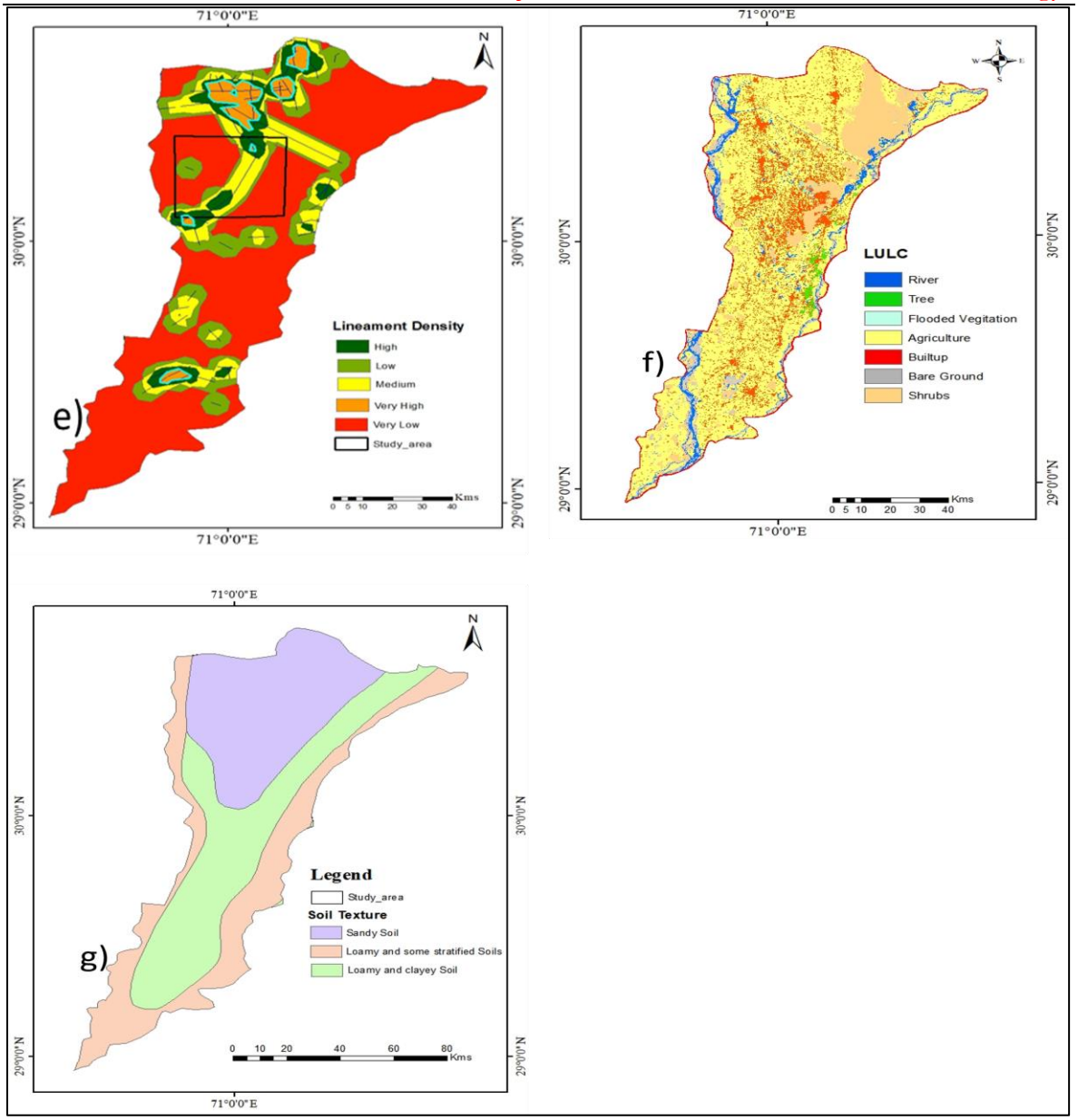

Figure 4: The map of thematic layers for Muzaffargarh, utilized in creating the GWPZ map, includes the study area indicated by a small black box. This figure comprises the following: a) Slope, b) Geology, c) Rainfall, d) Drainage Density, e) Lineament Density, f) Land Use/Land Cover (LULC), and g) Soil Classification Map.

Table 3: Interpretation of GG-01

Layer No.	Resistivity (Ohm-m)	Thickness (m)	Depth (m)	Interpretation	Remarks
1	3.91	1.21	1.21	Clay	The third, fourth, and fifth layers are water-bearing. Drilling is required for further investigation.
2	191	1.48	2.69	Gravel	
3	10.6	7.82	10.5	Saline sediments	
4	66.6	45.7	56.2	Medium to coarse grain sand with fresh groundwater	

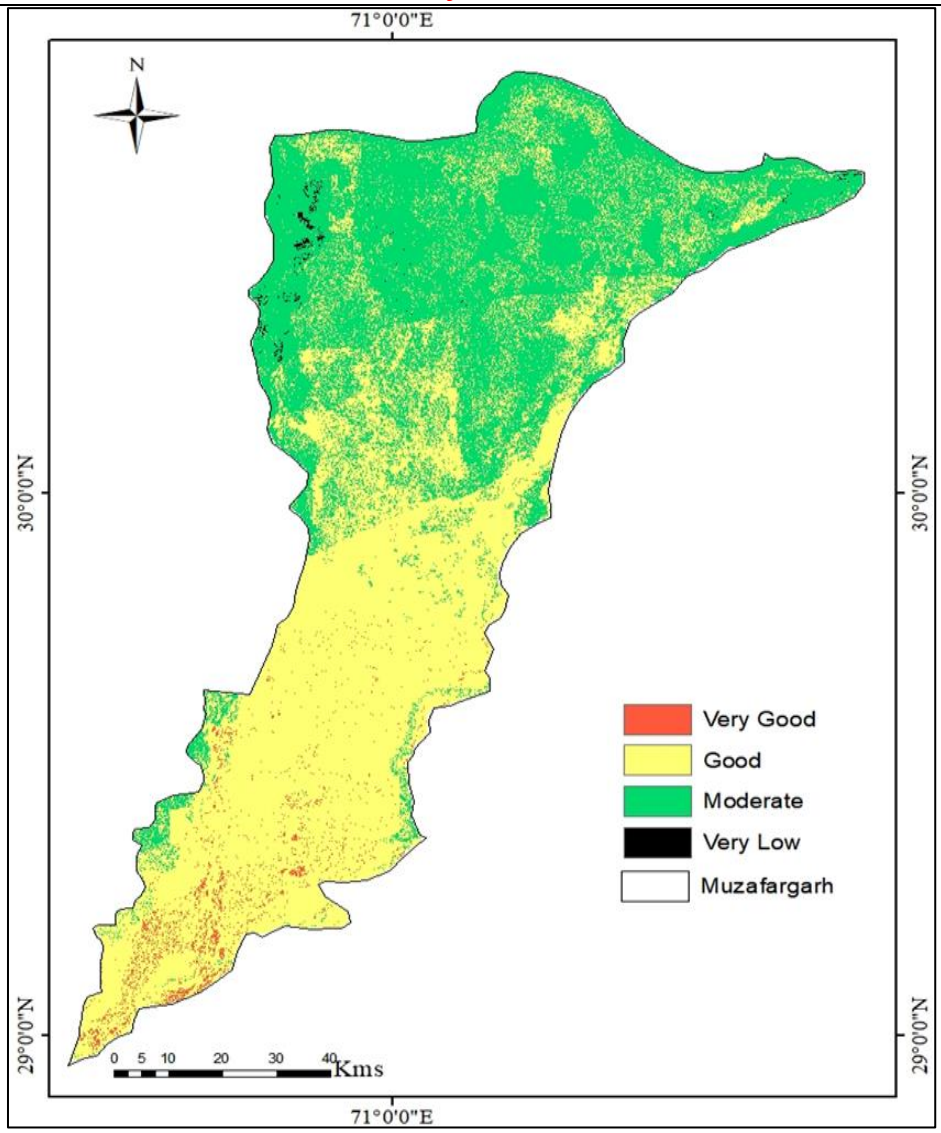

Figure 5: Groundwater Potential Zone Map of Muzaffargarh, it classifies the area into four groundwater quality zones: Very Good, Good, Moderate, and Very Low.

Interpretation of some of points is given below:

Table 4: Interpretation of KA-04

Layer No.	Resistivity (Ohm-m)	Thickness (m)	Depth (m)	Interpretation	Remarks
1	20.6	0.964	0.964	Clay or silt	The second and third layers are water-bearing. Drilling is required for further investigation
2	34.3	39.2	40.1	Clay or silty clay or clayey silt saturated with water	
3	51.6			Medium to coarse grain sand with fresh groundwater	

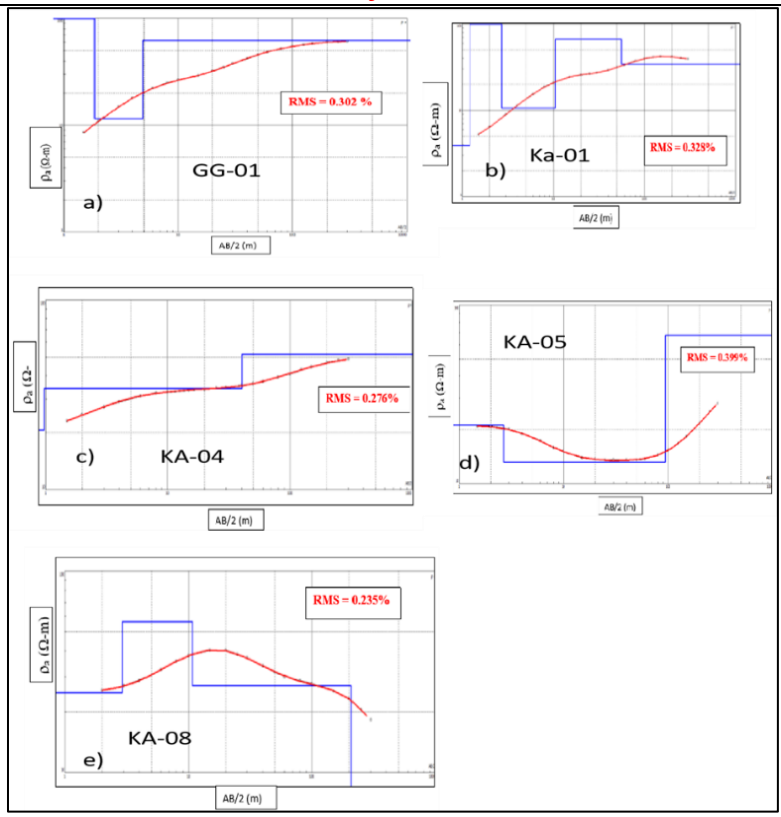

Figure 6: 1D inverted models of apparent resistivity data are indicated by small circles. The solid black curve represents the apparent resistivity curve, while the red curve is the best fit to this data. The solid blue block line shows the modeled (synthetic) resistivity. The horizontal axis represents the current electrode spacing (AB/2) in meters, and the vertical axis shows the resistivity in ohm meters. The figure includes the following plots: a) GG-01, b) KA-01, c) KA-04, d) KA-05, and e) KA-08.

Table 5: Interpretation of KA-05

Layer No.	Resistivity (Ohm-m)	Thickness (m)	Depth (m)	Interpretation	Remarks
1	21.2	2.66	2.66	Clay or silt	The second and third layers are water-bearing. Drilling is required further.
2	13.2	92.2	94.9	Saline sediments	
3	67.9			Medium to coarse grain sand with fresh groundwater	

Table 6: Interpretation of KA-08

Layer No.	Resistivity (Ohm-m)	Thickness (m)	Depth (m)	Interpretation	Remarks
1	25	2.9	2.9	Clay or silt	
2	55.8	7.87	10.8	Medium to coarse grain sand with fresh groundwater	The second, third, and fourth layers are water-bearing.
3	27	198	209	Clay or silt with marginal water	Drilling is required for further
4	0.354			Saline sediments	

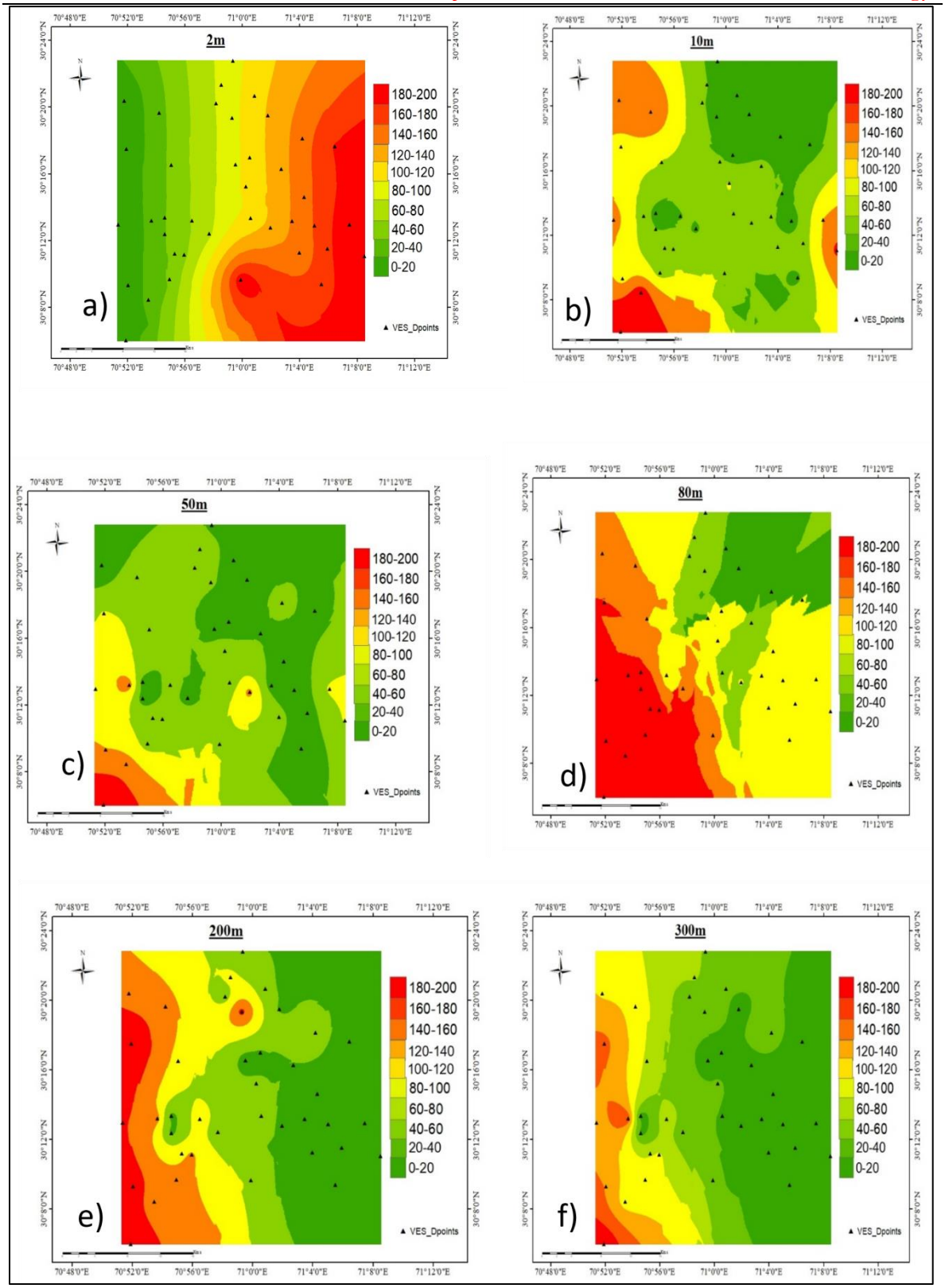

Figure 7: Contour map representing resistivity distribution at study area in Muzaffargarh at different depth i.e. a) 2m, b) 10m, c) 50m, d) 80m, e) 200m, f) 300m

Resistivity maps were generated at depth levels of 2 m, 10 m, 50 m, 80 m, 150 m, 200 m, and 300 m to analyze the variation in resistivity values in the Ghazi Ghat and Qasba Gujrat areas of the Muzaffargarh district. Clays and silty clay sediments present above the water table exhibit low resistivity values. Water-saturated sand sediments have resistivity values ranging from 40 to 100 ohmmeters. Saline sediments show low resistivity values both above and below the water table. The resistivity maps, created from ground data at various depths, illustrate groundwater quality and the variation in resistivity according to depth. These maps, shown in Figure 7, clearly depict the differences in water quality and resistivity at different locations.

Discussion:

Several studies have highlighted the risks associated with groundwater depletion due to agricultural use. In this study, approximately 40 observations of groundwater levels were conducted across different locations for resistivity modeling and groundwater mapping. Resistivity models were generated and plotted, displaying resistivity values against depths, and consisting of sequences of horizontal layers distinguished by discrete resistivity bands. Calibration between lithology and resistivity was established using provided information and resistivity data, as summarized in Table 2.

Interpreting the Vertical Electrical Sounding (VES) results in this region proved challenging due to similar resistivity readings between shallow and deep alluvial sediments. Sand and gravel sediments typically serve as good aquifers for fresh groundwater, while clay-rich sediments act as aquifers for saline water. Figure 6 presents various models where the red curves represent synthetic or best-fit curves for the field data, demonstrating a Root Mean Square Error (RMSE) of less than 1. These synthetic curves help minimize errors, with the blue lines indicating subsurface lithologies and their corresponding depths.

Figure 6a illustrates four subsurface layers: clay, gravelly sand, silt, and sand saturated with freshwater. Low resistivity values suggest saline water, while high resistivity values indicate freshwater. Figure 6b shows five geo-electric layers with distinct lithologies, including clay, gravel, saline sediments, medium to coarse-grained sand with freshwater, and water-saturated clay or silty clay. The coordinates for these layers are 30° 18′ 94″ N, 70° 94′ 97″ E. Figure 6c, located at 30° 13′ 11″ N, 70° 56′ 28″ E, depicts three lithologic layers: clay or silt (top layer), clay or silty clay saturated with water (middle layer), and medium to coarse-grained sand with freshwater (bottom layer). Figure 6d, at 30° 12′ 25″ N, 70° 57′ 40″ E, features three lithologic units: clay or silt (uppermost layer), saline sediments (second layer), and medium to coarse-grained sand with fresh groundwater (third layer). Figure 6e, located at 30° 13′ 21″ N, 71° 00′ 33″ E, shows four lithologic units: clay or silt (top layer), medium to coarse-grained sand with freshwater (second layer), clay or silt (third layer), and saline sediments (fourth layer).

In the study area, resistivity values are categorized as follows: very high (greater than 230 Ω-m), high (between 100 and 200 Ω-m), medium (between 40 and 100 Ω-m), low (between 20 and 40 Ω-m), and very low (less than 20 Ω-m). The electrical resistivity data reveal thick layers of Quaternary sediments in the subsurface, primarily composed of clay, silt, sand, and gravel. These resistivity values were determined from field data and plotted at various depths in ArcGIS. Resistivity maps were created at different depths, including 2 m, 10 m, 50 m, 80 m, 200 m, and 300 m, to analyze variations in resistivity. Figure 7 presents these maps, illustrating resistivity at different depths.

Figure 7a shows the resistivity map at a depth of 2 meters, primarily reflecting lithologic variations, with resistivity values ranging from less than 10 Ω-m to over 250 Ω-m. Sampling locations towards the west exhibit low resistivity values, suggesting alluvium or silty materials, while those towards the east show high resistivity values, indicating boulders or gravelly strata. Figure 7b displays resistivity at 10 meters, with medium to high resistivity values indicating freshwater, and values up to 40 Ω-m suggesting silty clay or clayey silt with brackish water.

Values below 10 Ω-m show saline sediments. Figure 7c illustrates resistivity distribution at 50 meters, with high to very high resistivity values (120-200 Ω-m) indicating freshwater, while other locations show low to medium resistivity. Figure 7d shows resistivity distribution at 80 meters, with a trend from low to high resistivity from east to west. Figures 7e and 7f indicate favorable locations for freshwater towards the west, with sand and gravel containing fresh and saline water.

Conclusion:

The study effectively employed Remote Sensing (RS), Geographic Information Systems (GIS), the Analytical Hierarchy Process (AHP), and electrical resistivity techniques to evaluate and identify potential groundwater zones. The research involved creating thematic layers, assigning weights using AHP, and performing overlay analysis to delineate groundwater potential zones. Electrical resistivity surveys revealed three to five geoelectric layers in the study area, including organic content, silty clay, fine to coarse sand, and gravel. Low resistivity values indicate saline water, while high values suggest freshwater. Sites with high resistivity, primarily consisting of gravelly sand, show potential for freshwater. Sites such as GG-01, GG-02, GG-03, GG-04, GG-05, GG-06, GG-07, GG-08, KA-01, KA-02, KA-03, KA-04, KA-05, KA-08, and KA-10 are recommended for test drilling.

Recommendations:

- Validate survey data with borehole information.
- Allocate a groundwater budget for water management in underdeveloped areas.
- Conduct groundwater quality surveys every five years under the Ministry of Water and Power's supervision.
- Utilize vertical electrical sounding, electrical resistivity tomography, and seismic refraction techniques for result verification.
- Ensure public accessibility to borehole data in underdeveloped areas.
- Launch a government awareness campaign on the importance of quality water.
- Obtain government approval before installing new water tube wells.

Acknowledgement: I, the First Author, declare that this manuscript is original, has not been published before and is not currently being considered for publication elsewhere.

Author's Contribution: W.S. proposed the topic and S.A and M.U. modified the topic. P.K. helped to gather data from field. W.S. handled the data processing, data analysis, and wrote the whole manuscript. S.G. and S.A. helped with the enhancement of the research design, data analysis, interpretation, and manuscript writing. S.A. finalized, reviewed and edited the manuscript. All authors read and agreed to the published version of the manuscript.

Conflict of Interest: The authors have declared no conflict of interest.

References:

[1] M. Hasan, Y. Shang, P. Shao, X. Yi, and H. Meng, "Evaluation of Engineering Rock Mass Quality via Integration Between Geophysical and Rock Mechanical Parameters," Rock Mech. Rock Eng., vol. 55, no. 4, pp. 2183–2203, Apr. 2022, doi: 10.1007/S00603-021-02766-8/METRICS.

[2] N. A. Bowling, "Is the job satisfaction–job performance relationship spurious? A meta-analytic examination," J. Vocat. Behav., vol. 71, no. 2, pp. 167–185, Oct. 2007, doi: 10.1016/J.JVB.2007.04.007.

[3] K. Rasool, M. Helal, A. Ali, C. E. Ren, Y. Gogotsi, and K. A. Mahmoud, "Antibacterial Activity of Ti3C2Tx MXene," ACS Nano, vol. 10, no. 3, pp. 3674–3684, Mar. 2016, doi:

10.1021/ACSNANO.6B00181/ASSET/IMAGES/NN-2016-00181G_M002.GIF.

[4] K. Indhulekha, K. C. Mondal, and D. C. Jhariya, "Groundwater prospect mapping using remote sensing, GIS and resistivity survey techniques in Chhokra Nala Raipur district, Chhattisgarh, India," J. Water Supply Res. Technol., vol. 68, no. 7, pp. 595–606, Nov. 2019, doi: 10.2166/AQUA.2019.159.

[5] S. Muhammad, M. I. Ehsan, and P. Khalid, "Optimizing exploration of quality groundwater through geophysical investigations in district Pakpattan, Punjab, Pakistan," Arab. J. Geosci. 2022 158, vol. 15, no. 8, pp. 1–15, Apr. 2022, doi: 10.1007/S12517-022-09990-8.

[6] P. Anbazhagan, M. Sreenivas, B. Ketan, S. S. R. Moustafa, and N. S. N. Al-Arifi, "Selection of Ground Motion Prediction Equations for Seismic Hazard Analysis of Peninsular India," J. Earthq. Eng., vol. 20, no. 5, pp. 699–737, Jul. 2016, doi: 10.1080/13632469.2015.1104747.

[7] K. Pratap, K. V. Ravindran, and B. Prabakaran, "Groundwater prospect zoning using remote sensing and geographical information system: A case study in Dala-Renukoot area, Sonbhadra district, Uttar Pradesh," J. Indian Soc. Remote Sens., vol. 28, no. 4, pp. 249–263, 2000, doi: 10.1007/BF02990815/METRICS.

[8] R. K. Prasad, N. C. Mondal, P. Banerjee, M. V. Nandakumar, and V. S. Singh, "Deciphering potential groundwater zone in hard rock through the application of GIS," Environ. Geol., vol. 55, no. 3, pp. 467–475, Aug. 2008, doi: 10.1007/S00254-007-0992-3/METRICS.

[9] B. Deepika, K. Avinash, and K. S. Jayappa, "Integration of hydrological factors and demarcation of groundwater prospect zones: Insights from remote sensing and GIS techniques," Environ. Earth Sci., vol. 70, no. 3, pp. 1319–1338, Oct. 2013, doi: 10.1007/S12665-013-2218-1/METRICS.

[10] K. C. Ng et al., "Experimental investigation of the silica gel–water adsorption isotherm characteristics," Appl. Therm. Eng., vol. 21, no. 16, pp. 1631–1642, Nov. 2001, doi: 10.1016/S1359-4311(01)00039-4.

[11] S. Ali, D. Li, F. Congbin, and F. Khan, "Twenty first century climatic and hydrological changes over Upper Indus Basin of Himalayan region of Pakistan," Environ. Res. Lett., vol. 10, no. 1, p. 014007, Jan. 2015, doi: 10.1088/1748-9326/10/1/014007.

[12] M. T. Chan, A. Selvam, and J. W. C. Wong, "Reducing nitrogen loss and salinity during 'struvite' food waste composting by zeolite amendment," Bioresour. Technol., vol. 200,

pp. 838–844, Jan. 2016, doi: 10.1016/J.BIORTECH.2015.10.093.

[13] J. S. Singh, S. Koushal, A. Kumar, S. R. Vimal, and V. K. Gupta, "Book Review: Microbial Inoculants in Sustainable Agricultural Productivity- Vol. II: Functional Application," Front. Microbiol., vol. 7, p. 232116, Dec. 2016, doi: 10.3389/FMICB.2016.02105.

[14] B. K. Allam, N. Musa, A. Debnath, U. L. Usman, and S. Banerjee, "Recent developments and application of bimetallic based materials in water purification," Environ. Challenges, vol. 5, p. 100405, Dec. 2021, doi: 10.1016/J.ENVC.2021.100405.

[15] S. Niwas and O. A. L. De Lima, "Aquifer Parameter Estimation from Surface Resistivity Data," Groundwater, vol. 41, no. 1, pp. 94–99, Jan. 2003, doi: 10.1111/J.1745-6584.2003.TB02572.X.

[16] P. D. Sreedevi, K. Subrahmanyam, and S. Ahmed, "The significance of morphometric analysis for obtaining groundwater potential zones in a structurally controlled terrain," Environ. Geol., vol. 47, no. 3, pp. 412–420, Feb. 2005, doi: 10.1007/S00254-004-1166-1/METRICS.

[17] S. Y. ©1 and K. Elangovan, "Groundwater potential zones delineation using geo-electrical resistivity method and GIS for Coimbatore, India," IJMS Vol.47(05) [May 2018], vol. 47, no. 05, pp. 1088–1095, 2018, Accessed: Jun. 15, 2024. [Online]. Available: http://nopr.niscpr.res.in/handle/123456789/44408

[18] M. A. Hagras and A. F. Agamy, "The effect of downstream perforated blanket on the safety against piping in heading-up structures," Ain Shams Eng. J., vol. 5, no. 1, pp. 41–47, Mar. 2014, doi: 10.1016/J.ASEJ.2013.07.008.

[19] D. W. Greenman, W. V. Swarzenski, and G. D. Bennett, "Ground-water hydrology of the Punjab region of West Pakistan, with emphasis on problems caused by canal irrigation," Water Supply Pap., 1967, doi: 10.3133/WSP1608H.

[20] P. W. Swarzenski, C. D. Reich, R. M. Spechler, J. L. Kindinger, and W. S. Moore, "Using multiple geochemical tracers to characterize the hydrogeology of the submarine spring off Crescent Beach, Florida," Chem. Geol., vol. 179, no. 1–4, pp. 187–202, Sep. 2001, doi: 10.1016/S0009-2541(01)00322-9.

[21] R. T. Nickson, J. M. McArthur, B. Shrestha, T. O. Kyaw-Myint, and D. Lowry, "Arsenic and other drinking water quality issues, Muzaffargarh District, Pakistan," Appl. Geochemistry, vol. 20, no. 1, pp. 55–68, Jan. 2005, doi: 10.1016/J.APGEOCHEM.2004.06.004.

[22] M. S. E. Juanah, S. Ibrahim, W. N. A. Sulaiman, and P. A. Latif, "Groundwater resources assessment using integrated geophysical techniques in the southwestern region of Peninsular Malaysia," Arab. J. Geosci., vol. 6, no. 11, pp. 4129–4144, Nov. 2013, doi: 10.1007/S12517-012-0700-9/METRICS.

[23] A. Maqsoom et al., "Landslide susceptibility mapping along the China Pakistan Economic Corridor (CPEC) route using multi-criteria decision-making method," Model. Earth Syst. Environ., vol. 8, no. 2, pp. 1519–1533, Jun. 2022, doi: 10.1007/S40808-021-01226-0/METRICS.

[24] T. Melese and T. Belay, "Groundwater Potential Zone Mapping Using Analytical Hierarchy Process and GIS in Muga Watershed, Abay Basin, Ethiopia," Glob. Challenges, vol. 6, no. 1, p. 2100068, Jan. 2022, doi: 10.1002/GCH2.202100068.

[25] K. Ashwini, R. K. Verma, S. Sriharsha, S. Chourasiya, and A. Singh, "Delineation of groundwater potential zone for sustainable water resources management using remote sensing-GIS and analytic hierarchy approach in the state of Jharkhand, India," Groundw. Sustain. Dev., vol. 21, p. 100908, May 2023, doi: 10.1016/J.GSD.2023.100908.

[26] M. Rajesh, E. Kavaz, and D. P. R. B., "Photoluminescence, radiative shielding properties of Sm3+ ions doped fluoroborosilicate glasses for visible (reddish-orange) display and radiation shielding applications," Mater. Res. Bull., vol. 142, p. 111383, Oct. 2021, doi: 10.1016/J.MATERRESBULL.2021.111383.